catalysts

MDPI

Article

Poisoning of Ammonia Synthesis Catalyst Considering Off-Design Feed Compositions

Alireza Attari Moghaddam [1] and Ulrike Krewer [1,2]*

[1] Institute of Energy and Process Systems Engineering, TU Braunschweig, 38106 Braunschweig, Germany; a.a.moghaddam@tu-braunschweig.de
[2] Institute for Applied Materials, Karlsruhe Institute of Technology, 76131 Karlsruhe, Germany
* Correspondence: ulrike.krewer@kit.edu; Tel.: +49-721-6084-7491

Received: 1 September 2020; Accepted: 30 September 2020; Published: 22 October 2020

Abstract: Activity of ammonia synthesis catalyst in the Haber-Bosch process is studied for the case of feeding the process with intermittent and impurity containing hydrogen stream from water electrolysis. Hydrogen deficiency due to low availability of renewable energy is offset by increased flow rate of nitrogen, argon, or ammonia, leading to off-design operation of the Haber-Bosch process. Catalyst poisoning by ppm levels of water and oxygen is considered as the main deactivation mechanism and is evaluated with a microkinetic model. Simulation results show that catalyst activity changes considerably with feed gas composition, even at exceptionally low water contents below 10 ppm. A decreased hydrogen content always leads to lower poisoning of the catalyst. It is shown that ammonia offers less flexibility to the operation of Haber-Bosch process under fluctuating hydrogen production compared to nitrogen and argon. Transient and significant changes of catalyst activity are expected in electrolysis coupled Haber-Bosch process.

Keywords: ammonia synthesis; power-to-ammonia; microkinetic model; catalyst deactivation; Haber-Bosch process; partial load

1. Introduction

Use of intermittent renewable energy (RE) sources, like solar and wind power, causes an imbalance between electricity supply and demand. One way to deal with this, is to convert surplus electrical energy produced from renewable sources into chemical energy for energy storage. The molecules should be preferably carbon-free liquid fuels, and their chemical energy should be easily convertible back into electricity on demand (power-to-x-to-power) [1]. This would enable better geographical accessibility to power through the transport of RE in the form of liquid fuels or through decentralized power-to-x-to-power units. Therefore, small and simple chemicals with high energy density are required, so that storage and transportation costs are kept low. In recent years, among energy-dense carbon-neutral liquid fuels, ammonia and its production from renewable resources, known as power-to-ammonia, has gained special attention [2,3]. Production of ammonia from renewables has been the subject of many research projects leading to a steep increase in the number of related publications in recent years, as seen in Figure 1.

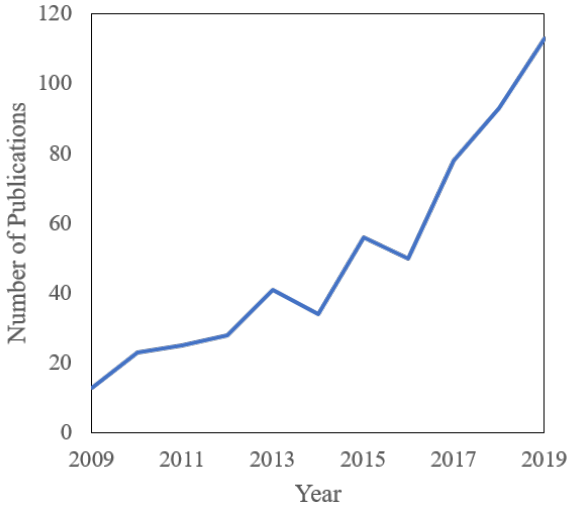

Figure 1. Annual number of publications returned from a scopus search using "renewable ammonia production" as keyword.

Ammonia is globally the second most produced inorganic chemical and it is mainly used for fertilizer applications. The industrial large-scale method for ammonia production is the Haber-Bosch (HB) process, in which nitrogen and hydrogen at high pressure and temperature and in the presence of an iron-based catalyst react to produce ammonia as

$$N_2(g) + 3H_2(g) \rightleftharpoons 2NH_3(g) \quad (1)$$

Equation (1) is an equilibrium reaction due to the high reactor temperature and as a result its reactants cannot be fully converted in one pass through the catalyst bed. Therefore, the unreacted nitrogen and hydrogen are sent back to the reactor inlet through a recycle loop. During the continuous process inert argon, water vapor and oxygen may enter the reactor as impurities from N_2 and H_2 production units. Water vapor and oxygen are poisons to the catalyst and therefore their concentration is kept at few ppms in the loop e.g., common oxygen equivalent concentration in the feed is up to 10 ppm [4]. Usually, the molar ratio of hydrogen to nitrogen (H:N) in the synthesis loop is adjusted to a stoichiometric ratio of 3:1 to ensure conversion close to equilibrium [5].

In the conventional HB plant, hydrogen production is the most energy-intensive step, which mainly uses fossil fuels like natural gas or coal as fuel and feedstock [1]. Today's technology of Haber-Bosch process is responsible for over 1 % of global energy-related CO_2 emissions [1]. Therefore, two aspects are expected in the future ammonia production plans: carbon emission mitigation during its production, and ammonia synthesis for energy storage. The recent advances in hydrogen production technology from water electrolysis comprises both above mentioned trends by coupling water electrolysis with Haber-Bosch process. The main difference compared to the conventional process is the production of hydrogen from water via water electrolysis, while the power required for the whole HB process is supplied by renewable energy. Another potential deviation from the conventional HB process based on steam reforming could be the addition of an air separation unit for the production of nitrogen in the electrolysis coupled HB. However, when using solid oxide electrolysers, the air separation unit may not be needed, as suggested by [6].

In the electrolysis coupled HB, a direct consequence of fluctuations of RE is that the reactants, especially hydrogen, may not be produced at their required minimum flow rate. Therefore, the reactor operation needs to be flexible to damp such intermittencies. It has been shown in [7,8] that nitrogen, inert gas or ammonia can be used to compensate the shortage of hydrogen and keep the pressure inside the synthesis loop sufficiently high. Similar effects were shown by modelling; especially,

increasing nitrogen and argon proved to be effective [9]. However, regular changes in operating point and feed composition can affect the performance of the catalyst [10,11].

The most common mechanisms of deactivation of ammonia catalyst in the electrolysis coupled HB process are poisoning by O_2 and H_2O and sintering [12]. Catalyst deactivation through poisoning is caused by the occupation of active sites of the catalyst by atomic oxygen and is highly affected by the interplay between gas molecules and adsorbed species at the catalyst surface [13]. This implies that catalyst poisoning would undergo a dynamic behaviour in varying conditions of the electrolysis coupled HB process. It has been shown that equivalent concentrations of oxygen and water vapor lead to the same degree of poisoning, presumably because as soon as oxygen is exposed to the catalyst it is converted into water [14]. Therefore, the actual poison present in the operating ammonia converter is H_2O. In regard to sintering, it seems that it is a consequence of substantial oxygen poisoning [4]. This means that poisoning through H_2O is the main deactivation mechanism of ammonia catalyst.

Despite the importance of poisoning of the iron catalyst by water vapor in ammonia synthesis, there have not been many studies on this topic. Especially, the mechanism of poisoning by water vapor has not been thoroughly investigated. This is mainly attributed to the difficulties encountered in UHV (Ultra High Vacuum) experiments of O_2 chemisorption, which are designed to determine the heat of oxygen chemisorption [13]. Also the fact that the catalyst is poisoned at very low ppm amounts of oxygenates makes it more difficult to perform experiments with high accuracy. The previous researches on the poisoning of iron catalyst mainly focus on the "basic observations" of this phenomenon. Among these are: equivalent effect of oxygenates (H_2O, O_2, CO, CO_2) on the degree of poisoning [14,15], sudden promotion of the synthesis rate as a result of puls injection of water vapor to the gas stream [16–18], or the reversibility of the oxygenate poisoning [17,19]. A comprehensive review of studies on poisoning of ammonia catalysis has been given in [20].

The aim of this article is to go beyond these studies and expand our knowledge on the poisoning degree of the ammonia synthesis catalyst at different operating conditions and gas compositions. This is especially of great importance for the operation of dynamic Haber-Bosch process in power-to-ammonia, where operating conditions and gas composition are exposed to significant variations. We will explicitly try to find out how and in what extent hydrogen shortage can be compensated by different gases present in the process and investigate their effect on the poisoning of the catalyst. It will also be shown whether a single equation, which is based on the macroscopic parameters of the process could provide reliable catalyst activities at different operating conditions and gas compositions.

Model-based microkinetic analysis of chemical reactions has proven to be a proper tool to predict the catalyst poisoning and reaction rate, as it looks at the microscopic interactions of adsorbed species at the catalyst surface or with the bulk flow [21,22]. The microkinetic mechanism of NH_3 synthesis from nitrogen and hydrogen on an iron-based catalyst and its poisoning by water vapor has already been developed and successfully validated with industrial data [12,13]. Therefore, it is regarded as a reliable tool to predict the synthesis rate and is used in this work for the first time to investigate the effect of gas composition on the activity of the catalyst.

The paper is organized as follows: the microkinetic model and the method to calculate the activity of the catalyst is discussed in the next section. After this, the simulation results at different temperatures and gas compositions on a single catalyst particle and over a catalyst bed are presented. The main conclusions are then summarized in the last section.

2. Mathematical Model

The most widely accepted microkinetic ammonia synthesis mechanism on promoted iron catalyst is presented by Stoltze [13], in which nitrogen and hydrogen go through the following elementary steps to produce ammonia:

$$N_2(g) + * \rightleftharpoons N_2* \tag{2}$$
$$N_2 * + * \rightleftharpoons 2N* \tag{3}$$
$$N * + H* \rightleftharpoons NH * + * \tag{4}$$
$$NH * + H* \rightleftharpoons NH_2 * + * \tag{5}$$
$$NH_2 * + H* \rightleftharpoons NH_3 * + * \tag{6}$$
$$NH_3* \rightleftharpoons NH_3(g) + * \tag{7}$$
$$H_2(g) + 2* \rightleftharpoons 2H* \tag{8}$$

where $*$ is a free active site on the catalyst surface. Adsorbed species on the surface are marked as well by $*$. The catalytic reaction is assumed to be at quasi-equilibrium, meaning that equilibrium equations are used for all but the slowest step [21]. Here the second step is the slowest or rate-determining step (RDS) [23].

The catalyst is considered to be deactivated through the poisoning by water vapor. This can be described by the following fast elementary reaction [13]

$$H_2O(g) + * \rightleftharpoons H_2(g) + O* \tag{9}$$

The interaction of inert argon with the active sites of the catalyst is neglected. The set of reaction Equations (2) to (9) has been validated against reactor data and can well describe the surface kinetics of ammonia synthesis and catalyst poisoning [13]. For the microkinetic model formal kinetic equilibrium equations are used for each of the fast elementary reactions and deactivation:

$$K_1 = k_{1f}/k_{1b} = \theta_{N_2}/(p_{N_2}\theta_*) \tag{10}$$
$$K_3 = k_{3f}/k_{3b} = \theta_{NH}\theta_*/(\theta_N\theta_H) \tag{11}$$
$$K_4 = k_{4f}/k_{4b} = \theta_{NH_2}\theta_*/(\theta_{NH}\theta_H) \tag{12}$$
$$K_5 = k_{5f}/k_{5b} = \theta_{NH_3}\theta_*/(\theta_{NH_2}\theta_H) \tag{13}$$
$$K_6 = k_{6f}/k_{6b} = p_{NH_3}\theta_*/\theta_{NH_3} \tag{14}$$
$$K_7 = k_{7f}/k_{7b} = \theta_H^2/(p_{H_2}\theta_*^2) \tag{15}$$
$$K_8 = k_{8f}/k_{8b} = p_{H_2}\theta_O/(p_{H_2O}\theta_*) \tag{16}$$

where k_f, k_b, K, θ, and p are forward and backward rate constants, equilibrium constant, surface coverage and pressure, respectively. The rate constant is calculated from Arrhenius equation $k = k_0\, exp(-E_a/RT)$, where k_0, E_a, R and T are pre-exponential factor, activation energy, ideal gas constant and temperature, respectively. For the rate-determining step the formal kinetic rate equation is used

$$r_2 = k_{2f}\theta_{N_2}\theta_* - k_{2b}\theta_N^2 \tag{17}$$

in which r_2 is based on the number of turnovers per site per time. At the surface of the catalyst, the total coverage of adsorbed species is equal to the occupied active sites

$$1 - \theta_* = \theta_{N_2} + \theta_N + \theta_{NH} + \theta_{NH_2} + \theta_{NH_3} + \theta_H + \theta_O \tag{18}$$

Using Equations (10) to (16) to describe θ_N and θ_{N_2} as a function of θ_*, r_2 in Equation (17) can be rewritten as

$$r_2 = k_{2f}K_1(p_{N_2} - p_{NH_3}^2/(K_{eq}p_{H_2}^3))\theta_*^2 \tag{19}$$

in which K_{eq} is the equilibrium constant of the gas phase and is calculated as $K_{eq} = K_1 \cdot K_2 \cdot K_3^2 \cdot K_4^2 . K_5^2 \cdot K_6^2 \cdot K_7^3$. The activity of the catalyst can be expressed as

$$\alpha = \frac{r}{r_0} \tag{20}$$

in which r_0 and r are the reaction rate in the absence and presence of poisoning agents at similar operating conditions and gas composition, respectively. Combining two previous equations and assuming ppm concentration of water in the poisonous gas, the activity of the catalyst can then be expressed as a function of surface coverages as

$$\alpha = (\frac{\theta_*}{\theta_{*0}})^2 \tag{21}$$

where θ_{*0} and θ_* is the free surface coverage in the absence and presence of water, respectively. Dividing Equation (18) over surface coverage of free sites and rearranging the equation, we get

$$\frac{1}{\theta_{*0}} + \frac{\theta_O}{\theta_*} = \frac{1}{\theta_*} \tag{22}$$

This allows us to express activity as a function of surface coverage of oxygen as

$$\alpha = (1 - \theta_O)^2 \tag{23}$$

The kinetic parameters of the above presented microkinetic model are taken from [13,24] for an industrial promoted iron catalyst with site density of 60 µmol/gr [24] and has been recalled in Table 1. The activity change on a catalyst bed is investigated by assuming that the synthesis gas is fed to an isothermal fixed-bed reactor filled with the catalyst, in which the radial flow is neglected. The diffusion resistance for mass transfer is also neglected. The nitrogen conversion profile over the catalyst bed is obtained by discretizing the reactor into 10,000 equidistant computational cells in axial dimension. The conversion of nitrogen at computational node i (i changes from 1 to 10,000) is calculated as

$$X_{N_2,i} = r_{2,i-1} N_s / (N_{AV} F_{N_2,i-1}) \tag{24}$$

where N_s, N_{AV} and F_{N_2} are the number of active sites of catalyst in each cell (constant for all cells), Avogadro number and molar flow rate of nitrogen, respectively. The mole fraction of gas components at computational nodes is determined by the mass conservation. For example for nitrogen we have

$$y_{N_2,i} = \frac{y_{N_2,i-1}(1 - X_{N_2,i})}{1 - 2X_{N_2,i} y_{N_2,i-1}} \tag{25}$$

The total molar flow rate of all gas components at node *i* can then be obtained as

$$F_i = \frac{F_{N_2,i-1}}{y_{N_2,i}}(1 - X_{N_2,i}) \tag{26}$$

Knowing the molar flow rates, the nodal partial pressure of each component can be calculated by the ideal gas law.

Table 1. Equilibrium and rate constants based on Arrhenius equation ($k' \, exp(-E'/RT)$) [13,24].

Parameter	k'	E' (kJ/mol)
K_1	1.3×10^{-8} bar^{-1}	−43.1
K_2	3.25	−126.5
k_{2f}	4.29×10^{9} s^{-1}	28.5
K_3	159.1	58.1
K_4	9.5	36.4
K_5	1.67	38.7
K_6	20,600 bar	39.2
K_7	2.1×10^{-7} bar^{-1}	−93.8
K_8	0.024	−117

A macroscopic equation for the prediction of catalyst activity is suggested by Andersen [12], which has been shown to successfully reproduce experimental measurements of activity for different gas compositions. This equation is regarded as the one of the most reliable macroscopic equations for the prediction of ammonia catalyst activity and is expressed as

$$\alpha = A + B\,T + C\,T\,ln(y_{H_2O}) \tag{27}$$

T and y_{H_2O} are temperature and mole fraction of water, respectively. It is expected that the coefficients of Equation (27), A, B and C, change with pressure and composition of the gas, knowing that the poisoning of the catalyst is affected by environmental conditions. Equation (27) states that the activity of the catalyst changes linearly with $ln(y_{H_2O})$ and T, provided all other conditions stay constant. Here, with the help of microkinetic simulations, the validity of Equation (27) and the dependency of its coefficients on environmental conditions for different compositions of the gas mixture will be assessed.

As mentioned in the introduction, a common oxygen equivalent concentration in the feed of the ammonia converter is up to 10 ppm [4]. In this study, three different concentrations of water for the simulations are considered: 5 and 10 ppm, which correspond to industrial applications, as well as 30 ppm, which is considered here as an extreme case to show the loss of catalyst activity, when the "standard" 10 ppm water is not maintained in the synthesis gas. The simulations will be first implemented to investigate the effect of temperature and gas composition on the iron catalyst activity. Afterwards, the mathematical model will be used on a catalyst bed to study ammonia synthesis and catalyst deactivation at different gas compositions.

3. Simulation Results and Discussion

3.1. Catalyst Activity as a Function of Temperature

In the first step, we analyse the change of activity as a function of temperature. Gas mixture is assumed to contain 5% ammonia and argon, while the volumetric ratio of H:N is 3:1, and pressure is 150 bar. The activity profiles for 5, 10 and 30 ppm water concentration in the inlet gas are shown in Figure 2. Surface coverage of the most important surface species, i.e., atomic nitrogen, hydrogen and oxygen, as well as free sites for all three water contents is plotted in Figure 3. As it is seen in these two figures, by increasing the temperature, the adsorbed oxygen ratio and consequently poisoning effect of water is significantly decreased. This is due to the fact that water adsorption (Equation (9)) is exothermic and slows down or reverses, as the temperature increases. This phenomenon is also being utilized in industrial plants to regain the activity of the used catalyst [20]. lAlso, the higher the water content in the synthesis gas the larger is the drop in catalyst activity, since more oxygen is adsorbed at the catalyst surface. This effect is very strong: at the same temperature, activity may change by 30% to 60%, see Figure 2. These results are in qualitative agreement with the results in [25].

The linear change of activity with temperature, suggested by Equation (27), cannot be confirmed for all temperatures, as seen in Figure 2. However, in the temperature range between 673–773 K,

which is mostly practiced in industrial applications, an almost linear dependency can be seen with a similar slope for different water concentrations. The y-intercept value, i.e., constant A in Equation (27), would then be a function of y_{H_2O}.

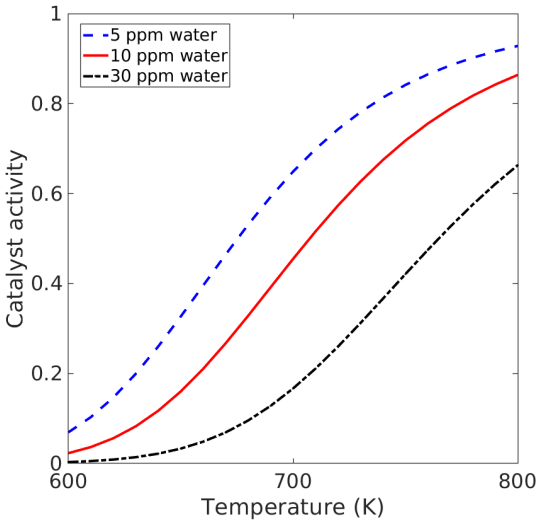

Figure 2. Catalyst activity as a function of temperature for different water concentrations in the gas mixture. P = 150 bar, H:N = 3, $y_{Ar} = 0.05$, $y_{NH_3} = 0.05$.

In the considered temperature range, the coverage of free sites is lower than for other species, as seen in Figure 3. This is beneficial, as in the industrial applications a low number of free sites is desired to achieve a higher synthesis rate and conversion of the reactants in a smaller volume of the catalyst. Another interesting point observed in this figure, is the weak adsorption of hydrogen on the iron catalyst compared to N and O. In fact, in the presence of water in the synthesis gas, the competition between nitrogen and oxygen for adsorption on the surface is the decisive factor for determining the reaction rate. For example, in the presence of 5 ppm water in the gas mixture, the surface coverage of nitrogen is greater than that of oxygen at temperatures higher than 640 K. For 30 ppm water, however, this would happen only at around 730 K. Since increasing temperature is costly on the one hand, and on the other hand could damage the catalyst, it is of vital importance to keep the concentration of water in the gas mixture as low as possible, preferably even significantly below 10 ppm, to be able to achieve higher activity values, while keeping the temperature low. In any case, it becomes clear also that catalyst studies without few ppm water will cause strongly different surface conditions as in practical Haber Bosch reactors, where typically 10 ppm water may be expected.

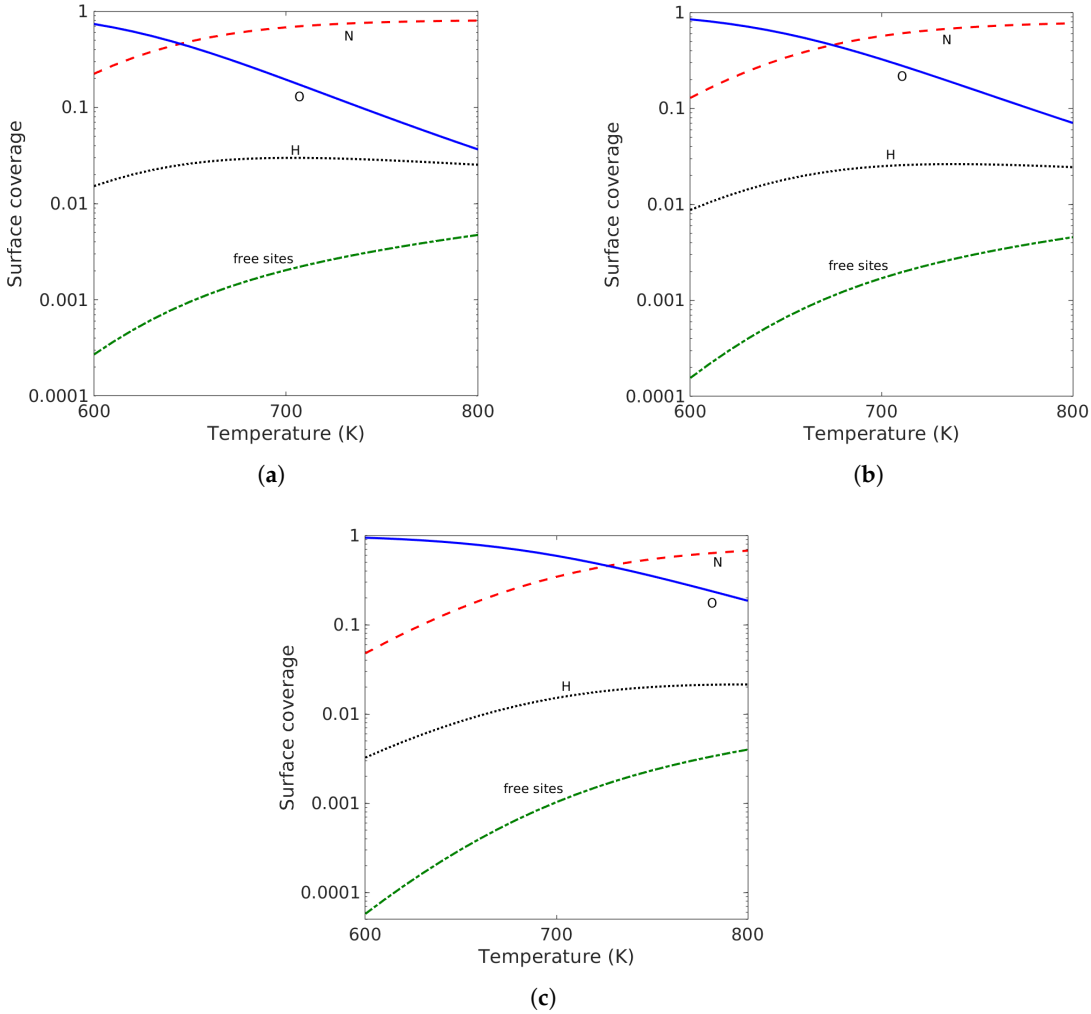

Figure 3. Surface coverage of atomic oxygen, nitrogen, hydrogen and free sites versus temperature. Pressure is 150 bar, H:N = 3:1, $y_{Ar} = 0.05$ and $y_{NH_3} = 0.05$. (**a**) 5 ppm water; (**b**) 10 ppm water; (**c**) 30 ppm water.

3.2. Catalyst Activity at Different Gas Compositions

As mentioned, in an electrolysis coupled HB plant, N_2, Ar or NH_3 are used to compensate for the shortage of hydrogen. Therefore, different gas compositions in the synthesis gas are expected. In this section, the effect of change of gas composition on the activity is analysed for low (5 ppm), medium (10 ppm) and high (30 ppm) water concentrations, while pressure and temperature are maintained at 150 bar and 700 K, respectively. In case of using extra nitrogen, the analysis will be made based on the volumetric ratio of hydrogen to nitrogen, H:N, whereas in case of using argon or ammonia, the activity results are based on the mole fraction.

In Figure 4a, catalyst activity is shown as a function of H:N with a constant total flow rate. This mimics the situation that the RE supply reduces, and thus hydrogen production rate drops. To keep the total flow rate constant, the nitrogen flow rate increases, reducing H:N from the optimal, stoichiometric ratio of 3:1. The smallest value for H:N in Figure 4a corresponds to $y_{H_2} = 0.15$ (H:N $\simeq$ 0.17), for which ammonia is not dissociated based on the equilibrium reaction.

As it is clear in Figure 4a, the activity of the catalyst increases slightly when decreasing H:N up to a ratio of close to around 1.2:1 and then rises rapidly with further decreasing H:N ratio. This effect holds for all concentrations of water and can be explained by the microkinetic model. With decreasing H:N ratio, the hydrogen partial pressure decreases, which leads to less amount of adsorbed hydrogen at the

surface, i.e., θ_H decreases. Therefore, equilibrium surface reactions involving θ_H will shift to the left to compensate the drop in θ_H, leading to the increase of atomic nitrogen at the surface. Consequently and since N and O are the most abundant species at the surface, oxygen concentration at the surface drops with decreasing H:N ratio, which improves the performance of the catalyst.

As hydrogen fraction in the gas mixture reduces, the state of the gas gets closer to equilibrium. The approach to equilibrium can be expressed by efficiency, which we define here as the ratio of amount of ammonia in the gas mixture to its equilibrium value. The efficiency of the gas mixture with 30 ppm water and varying H:N ratios is illustrated in Figure 5. As it is seen, when decreasing H:N from 1.2:1, the efficiency increases significantly, which is due to the decrease in the "effective" hydrogen to nitrogen amount. This results also in a much higher rate of change in atomic nitrogen at the surface and consequently a strongly decreased synthesis rate. At larger H:N above 1.2:1 there is still "enough" hydrogen in the gas mixture, to maintain a high reaction rate, keeping the nitrogen surface concentration low. This leads also to an almost constant adsorbed oxygen and catalyst activity.

Almost over the whole range of H:N and in case of 5 ppm water, approximately 20% of the active sites are occupied with oxygen, whereas oxygen covers nearly 30 and 60 percent of the catalyst surface for 10 and 30 ppm, respectively. This explains the shift to lower activity for increased water content, which is observed in Figure 4a.

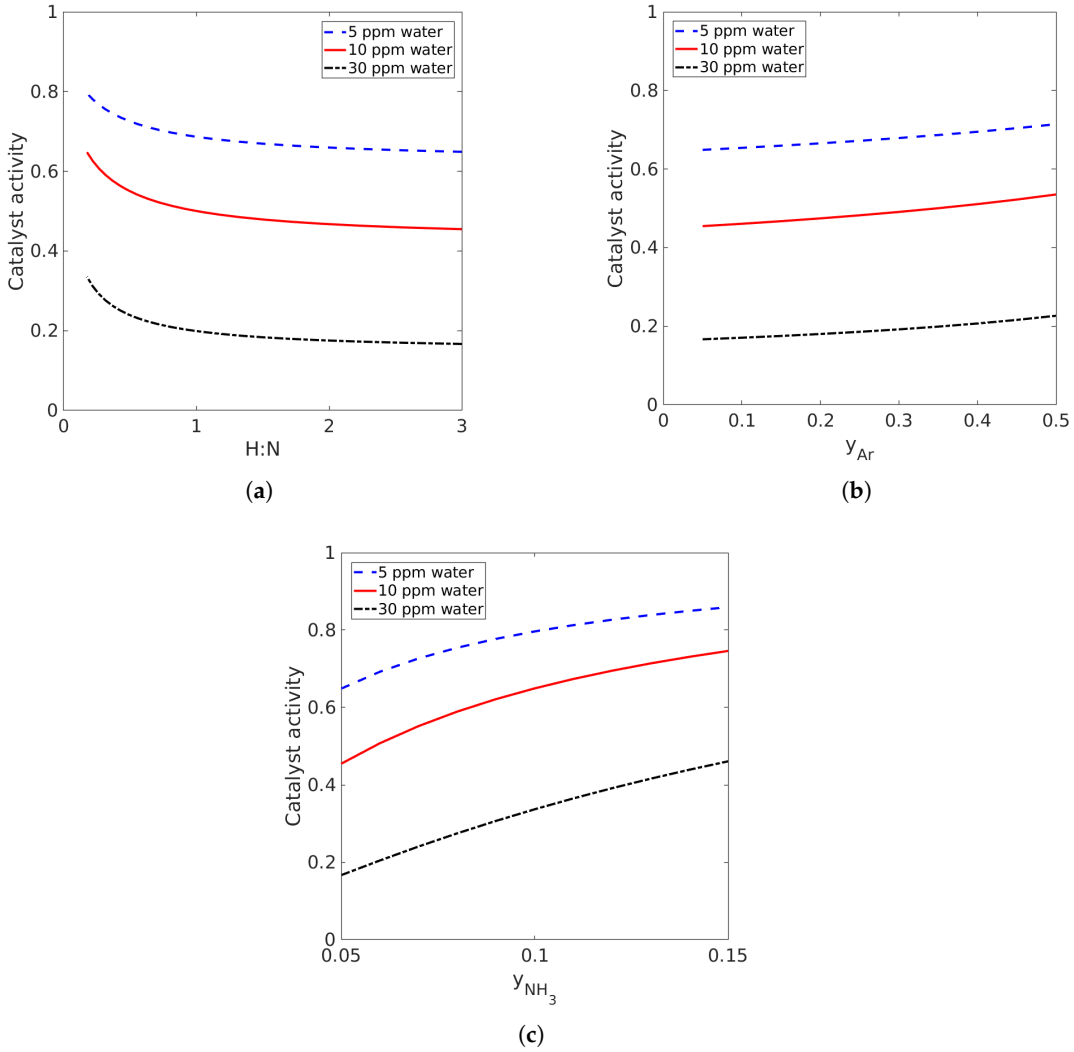

Figure 4. Catalyst activity for different gas compositions at P = 150 bar and T = 700 K. (**a**) $y_{Ar} = 0.05$, $y_{NH_3} = 0.05$; (**b**) H:N = 3, $y_{NH_3} = 0.05$; (**c**) H:N = 3, $y_{Ar} = 0.05$.

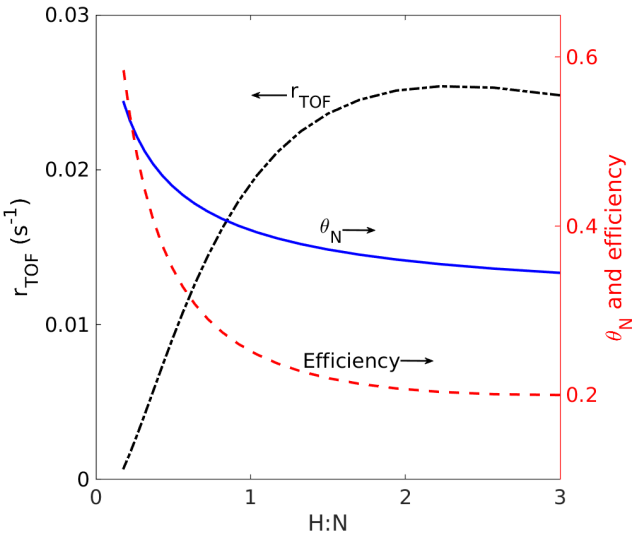

Figure 5. Change of intrinsic synthesis rate ($2r_2$), atomic adsorbed nitrogen and efficiency with H:N for 30 ppm water in a gas mixture with $y_{NH_3} = 0.05$, $y_{Ar} = 0.05$.

For using argon to compensate the shortage of hydrogen, we assume y_{Ar} can change from 0.05 to 0.5, while ammonia mole fraction stays at 0.05 and hydrogen to nitrogen molar ratio at the stoichiometric ratio of 3. In Figure 4b, change of catalyst activity as a function of mole fraction of Ar is shown. Increasing argon leads to slightly higher catalyst activity and decreased surface coverage by oxygen for all water concentrations. Increasing argon mole fraction at constant total pressure and hydrogen to nitrogen volumetric ratio means that the partial pressures of N_2 and H_2 and consequently θ_H and θ_{N_2} are decreased. This subsequently shifts equilibrium surface reactions involving θ_H and θ_{N_2} to the left, which finally leads to increasing atomic nitrogen at the surface. This effect is the same as for decreasing H:N ratios. As a result, less water is adsorbed with increasing y_{Ar} and catalyst becomes more active. It should be noted that Ar is of minor impact on activity, as activity changes only by 5% over the full range.

Finally, the change in the activity of the catalyst when increasing ammonia concentration for compensating the hydrogen shortage is shown in Figure 4c. In this case, the argon mole fraction is kept at 5% and volumetric ratio of hydrogen to nitrogen at 3:1, while mole fraction of ammonia changes from 0.05 to 0.15. The molar flow rate of ammonia in the synthesis loop cannot exceed a certain maximum, since due to the equilibrium reaction, ammonia will be dissociated into nitrogen and hydrogen. This means that, using only ammonia as the compensating gas for fluctuations in H_2 availability may not be sufficient to keep the flow rate of the synthesis loop above its minimum allowable flow rate. In this case, nitrogen or argon along with ammonia should be used to keep the flow rate high enough and avoid shutting down the reactor. It should be noted that there is no thermodynamic limitation in the concentration of nitrogen for compensating hydrogen shortage in the synthesis gas, and that for argon the limitation due to the equilibrium reaction exists also only at much lower hydrogen concentrations. Higher operational flexibility for Ar and H:N ratios compared to ammonia in Haber-Bosch process has been already shown in [9].

As shown in Figure 4c, the activity of the catalyst rises with ammonia concentration. The same trend is seen for all concentrations of water and can be attributed to the increase of atomic nitrogen concentration at the surface, as explained before in case of using extra argon or nitrogen. As a result, water is less adsorbed and concentration of oxygen at the surface is reduced. At lower ammonia mole fractions, surface composition and reaction rate are more sensitive to the changes in gas composition, since the gas phase is far from equilibrium. Below 10 ppm water content, this results in a sharper change of activity and θ_O with y_{NH_3} at low molar fractions of ammonia, whereas their variation becomes smoother as y_{NH_3} gets closer to its equilibrium value.

In order to assess the validity of Andersen's relationship on catalytic activity (Equation (27)) for different gas compositions, catalyst activity in the presence of 5 to 30 ppm water in the base case (H:N=3, $y_{Ar} = y_{NH_3} = 0.05$) is compared with three other cases, in each of which the composition of only one compensating gas is changed compared to the base case. The results are plotted in Figure 6. The black curve shows the activity of the base case, while the red, blue and green curves show the activity change when hydrogen shortage is compensated by argon, nitrogen and ammonia, respectively. The amount of drop of hydrogen content in the considered cases is not the same. In all of the four cases shown in Figure 6 and in agreement with Equation (27), the catalyst activity changes almost linearly with $ln(y_{H_2O})$ with identical slopes, except for the case in which extra ammonia is used (green curve) at low water content. Therefore, in case of using higher concentrations of nitrogen and argon in the synthesis gas, activity can be approximated by Equation (27), while the y-intercept (A + BT) must be expressed as a function of gas composition. The non-linear behavior of the ammonia case, the green curve, is due to the closer state of the gas phase to the equilibrium, as mentioned before.

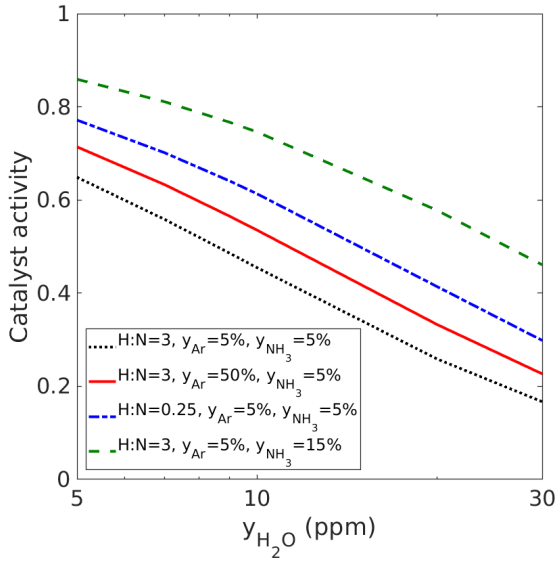

Figure 6. Change of catalyst activity for different gas compositions versus water content at P = 150 bar and T = 700 K.

Considering the activity dependency with temperature (Figure 2) and water content at different gas compositions (Figure 6), one could conclude that in general Andersen's equation describes these dependencies properly, however with some exceptions. For example, the linear dependency of activity with temperature is seen in a limited range of temperature. Also at water contents below around 10 ppm, and in case of using ammonia for compensation of hydrogen shortage, the activity does not obey the linear dependency with $ln(y_{H_2O})$. Moreover, in order to use this equation in variant conditions of gas mixture in power-to-ammonia, it is necessary to find the dependency of its coefficients, A, B and C, with operating conditions and gas compositions.An interesting point that can be observed in Figures 4 and 6 is that at each water content, by decreasing the hydrogen mole fraction, the catalyst activity increases for all compensating gases. Therefore, higher catalyst activities at the catalyst bed inlet are expected, when the hydrogen supply is reduced. Inside the catalyst bed, the composition of the gas along the bed changes and the activity will also locally vary. To identify the changes and effects inside the catalyst bed, a detailed mechanistic study is needed. This will be done in the next section.

3.3. Catalyst Activity Changes within the Catalyst Bed

To investigate the change of catalyst activity with the gas composition within a catalyst bed, the hydrogen content of the base case, the optimal operating point (H:N = 3, $y_{Ar} = y_{NH_3} = 0.05$), is decreased by 73%. This drop is then compensated firstly by nitrogen, leading to a volumetric ratio

of hydrogen to nitrogen equal to 0.25 in the gas stream. In the second case, the drop in hydrogen is offset by using both argon and nitrogen, which leads to a gas composition of H:N = 0.82 and $y_{Ar} = 0.55$. All three cases are passed isothermally through the catalyst bed with a space velocity of 12,000 1/hr, whereas temperature and pressure are 700 K and 150 bar, respectively. Catalyst weight is 6.25 g. The discretization and the mathematical formulations used can be found in the mathematical model section.

The activity profiles for all three gas streams in the presence of 5, 10 and 30 ppm water are plotted in Figure 7. The first observation is that the water content in the gas mixture plays an important role at all gas compositions on the activity of the catalyst. For example for the gas stream with H:N = 0.25, the average spatial activity is almost 0.8, 0.65 and 0.3 for 5, 10 and 30 ppm water, respectively. Based on Equation (23), this corresponds to almost 10%, 20% and 45% contamination of the catalyst surface with atomic oxygen, respectively. Significant poisoning of active surface sites with increasing only few ppm levels of water in the gas mixture shows again the importance of removing even traces of oxygen and water from the feed gas for the HB process.

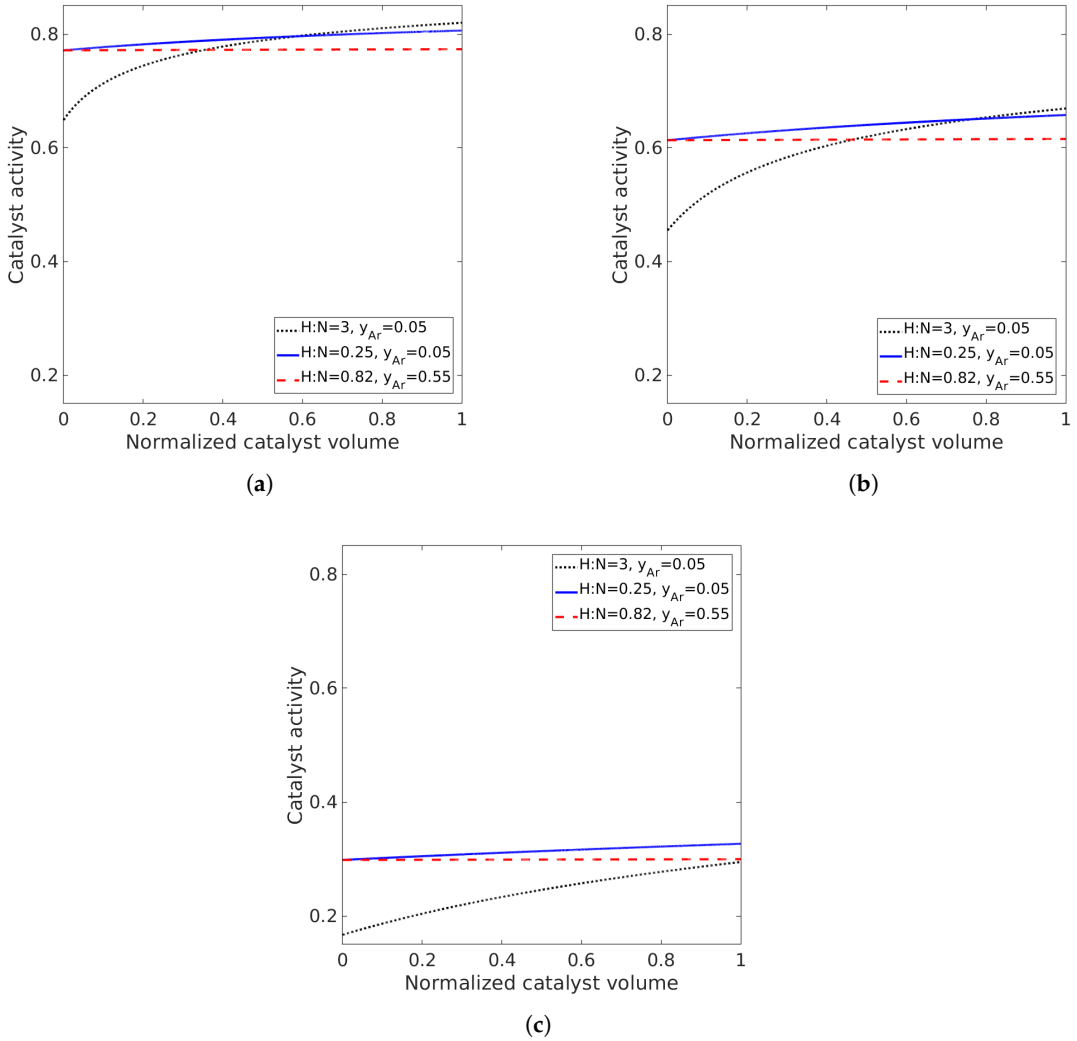

Figure 7. Change of catalyst activity along the catalyst bed for different gas compositions. (**a**) 5 ppm water; (**b**) 10 ppm water; (**c**) 30 ppm water.

The drop in the hydrogen content of the gas mixture reduces the synthesis rate, leading to a more uniform gas composition and consequently catalyst activity along the catalyst bed. To illustrate the influence of hydrogen content on the reaction rate, the local ratio of the reaction rates of low hydrogen

gas streams to that of the stoichiometric stream are plotted in Figure 8. Comparing the two subplots of this figure, it can be seen that the amount of the reduction of reaction rate as a result of lower hydrogen content depends on the gas composition. For example, for 10 ppm water in the gas mixture and in case of using only extra nitrogen for offsetting the hydrogen shortage, the drop in the reaction rate in the catalyst bed inlet is almost 13 times from that of the stoichiometric stream, whereas this value is almost 350 for the gas stream with the increased amount of both nitrogen and argon. The difference in the reaction rate of low hydrogen streams is mainly due to the closer state of the stream with H:N = 0.82 to equilibrium compared to the gas mixture with H:N = 0.25.

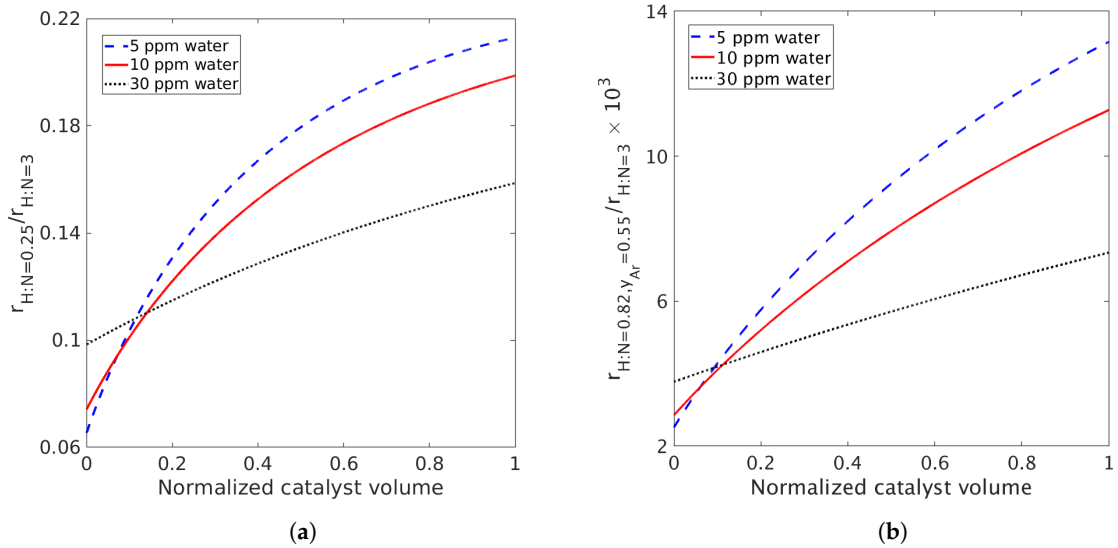

Figure 8. Ratio of reaction rate for the gas stream with only nitrogen (**a**) and both nitrogen and argon (**b**) as compensating gas for offsetting 73% drop in hydrogen supply.

As expected from the previous section, the activity at the reactor inlet for both cases with lower hydrogen content is higher. However, with moving inside the catalyst bed, and as the gas composition changes, the activity of low hydrogen streams may become smaller than that of the base case. The reason for this phenomenon is that the ammonia content of the stoichiometric case increases along the bed with a higher rate compared to the low hydrogen streams, since it is farther from the equilibrium state and has a higher synthesis rate. As a result, the catalyst activity enhances more rapidly (see Figure 4c) and may overtake the low hydrogen stream activities while moving forward inside the bed, as seen in Figure 7a,b. In the case of using simultaneous extra argon and nitrogen for compensating the hydrogen shortage, the spatial increase in activity along the catalyst bed is very small, whereas in case of using only nitrogen as the compensating gas, this increase is more pronounced, see Figure 7. This is observed for all levels of water content.

Another point that can be observed in both subplots of Figure 8 is that, higher amounts of water make the reaction rate ratios more uniform. This is because at higher water contents, the portion of poisoned active sites on the catalyst surface is higher (see Figure 3) and therefore, the synthesis rate is more limited to change with the gas composition.

The change of activity profile as a result of the variation in the gas composition means that there would be a transient change in the occupation of the catalyst surface by oxygen, which consequently affects the reaction rate. Since gas composition changes are expected to be more frequent in the electrolysis coupled HB process, predicting such transient behaviours, for example with a mathematical model based on first principles is vital to evaluate and optimize the performance of the process in real time.

4. Summary and Conclusions

Activity of an iron-based catalyst for the synthesis of ammonia in variant conditions of the electrolysis coupled HB process was studied. It was shown for all gas compositions that, increasing the water content by only few ppm's changes the activity of the catalyst significantly. For all levels of water content, the competition between adsorbed nitrogen and oxygen defined the activity of the catalyst. A higher water content reduces the occupation of active sites of the catalyst by nitrogen and consequently the activity decreases. It was also shown that temperature strongly affects the water adsorption and increasing it could reverse the poisoning of the catalyst by water. To achieve a high conversion of reactants in the ammonia converter, it is thus necessary to keep the water and oxygen content of the synthesis gas very low, preferably below 5 ppm.

A decreased hydrogen content lead to lower poisoning of the catalyst. However, the amount of reduction in catalyst poisoning for each compensating gas was different. When using ammonia to offset the shortage of hydrogen, the strongest activity variation with gas composition was observed. Also, ammonia could compensate a smaller amount of hydrogen shortage compared to argon and nitrogen, and as a result offers less flexibility in the operation of the electrolysis coupled HB reactor.

The validity of Andersen's macroscopic equation for the prediction of the activity at different operating conditions was also investigated. Comparing microkinetic simulation results with Andersen's equation, one could see that the linear dependency between activity and temperature is valid with a good approximation for industrially-relevant temperatures between 673 to 773 K. However, Andersen's equation does not consider the effect of gas composition on activity and therefore, needs to be revisited to include it. This could be accomplished with the help of the results presented in this work.

Simulation of ammonia synthesis over the catalyst bed for various inlet gas composition showed that the activity of the stoichiometric gas stream undertakes the biggest change along the catalyst bed, whereas the spatial variation of activity decreases, when the hydrogen content of the inlet gas reduces. The local activity of low hydrogen streams inside the bed could be bigger or smaller than that of the stoichiometric stream.

Change of the local activity with variation of inlet gas composition implies the local change of synthesis rate and the amount of heat released from the exothermic synthesis reaction. Therefore, for the robust operation of electrolysis coupled HB process, dynamic thermal measures must be considered, since cooling and heating of the catalyst bed play an important role in industrial ammonia reactors to achieve higher conversions and avoid hotspots [11,26]. For this, a dynamic model of the reactor, which consists of a reliable model for the prediction of activity in a wide range of operating conditions, as the one presented in this paper, could surely help to better manage such thermal effects.

Finally, it was illustrated that each compensating gas has some limitations and disadvantages in offsetting the hydrogen shortage, which is either due to the thermodynamics, kinetics or limited flexibility of the process. This suggests that there is no single answer that can be applied for all operating conditions and inlet gas compositions to the question of how the hydrogen shortage should be compensated in power-to-ammonia. Therefore, the best scenario for compensating the hydrogen shortage can be determined by investigating chemical and process-related implications of each scenario, for which catalyst activity plays a central role.

The results in this work contribute to better understanding of the flexibility of the dynamic HB process in power-to-ammonia. Flexibility of other power-to-chemical processes, which involve catalytic reactions, e.g., power-to-methanol [27], can also be investigated along the same lines as the present one. This work can also be extended to include the effect of temperature on the catalyst deactivation inside the bed, since temperature changes due to the exothermic ammonia synthesis reaction affect poisoning of the catalyst.

Author Contributions: Conceptualization, A.A.M. and U.K.; methodology, A.A.M.; software, A.A.M.; validation, A.A.M.; writing—original draft preparation, A.A.M.; writing—review and editing, A.A.M. and U.K.; supervision, U.K.; funding acquisition, U.K. All authors have read and agreed to the published version of the manuscript.

Funding: This work was done in the framework of the MOBILISE project (EW-3), financed by the state of Lower Saxony, Germany.

Acknowledgments: The publication of this article was funded by Technische Universität Braunschweig.

Conflicts of Interest: The authors declare no conflict of interest. The funders had no role in the design of the study; in the collection, analyses, or interpretation of data; in the writing of the manuscript, or in the decision to publish the results.

References

1. Philibert, C. (Ed.) *Renewable Energy for Industry*; IEA: Paries, France, 2017.
2. Nayak-Luke, R.; Bañares-Alcántara, R.; Wilkinson, I. "Green" Ammonia: Impact of Renewable Energy Intermittency on Plant Sizing and Levelized Cost of Ammonia. *Ind. Eng. Chem. Res.* **2018**, *57*, 14607–14616. [CrossRef]
3. Fuhrmann, J.; Hülsebrock, M.; Krewer, U. Energy Storage Based on Electrochemical Conversion of Ammonia. In *Transition to Renewable Energy Systems*; John Wiley & Sons, Ltd.: Hoboken, NJ, USA, 2013; Chapter 33, pp. 691–706.
4. Rase, H.F. (Ed.) *Handbook of Commercial Catalysts: Heterogeneous Catalysts*; CRC Press: Boca Raton, FL, USA, 2000.
5. Appl, M. Ammonia, 2. Production Processes. In *Ullmann's Encyclopedia of Industrial Chemistry*; John Wiley & Sons, Ltd.: Hoboken, NJ, USA, 2011.
6. Hansen, J.B. Solid Oxide Cell Enabled Ammonia Synthesis and Ammonia based Power Production. In Proceedings of the 14th Annual NH3 Fuel Conference, Minneapolis, MN, USA, 1–2 November 2017.
7. Ostuni, R.; Zardi, F. Method for Load Regulation of an Ammonia Plant. US Patent No. 2013/0108538 A1, 2 May 2013.
8. Kolbe, B.; Roosen, C.; Johanning, J.; Schulte Beerbühl, S.; Schultmann, F. Method and System for Producing a Product Gas under Changing Load Conditions. Patent No. WO 2017/153304 A1, 14 September 2017.
9. Cheema, I.I.; Krewer, U. Operating envelope of Haber-Bosch process design for power-to-ammonia. *RSC Adv.* **2018**, *8*, 34926–34936. [CrossRef]
10. Institute for Sustainable Process Technology (ISPT). *Power to Ammonia: Feasibility Study for the Value Chains and Business Cases to Produce CO_2-Free Ammonia Suitable for Various Market Applications*; ISPT: Amersfoort, The Netherlands, 2017.
11. Kalz, K.F.; Kraehnert, R.; Dvoyashkin, M.; Dittmeyer, R.; Gläser, R.; Krewer, U.; Reuter, K.; Grunwaldt, J.D. Future Challenges in Heterogeneous Catalysis: Understanding Catalysts under Dynamic Reaction Conditions. *ChemCatChem* **2017**, *9*, 17–29. [CrossRef] [PubMed]
12. Nielsen, P.E.H. Deactivation of Synthesis Catalyst. In *Catalytic Ammonia Synthesis, Fundamentals and Practice*; Jennings, J., Ed.; Springer: Berlin/Heidelberg, Germany, 1991; Chapter 8, pp. 285–301.
13. Stoltze, P. Surface science as the basis for the understanding of the catalytic synthesis of ammonia. *Phys. Scr.* **1987**, *36*, 824–864. [CrossRef]
14. Nielsen, A. *An Investigation on Promoted Iron Catalysts for the Synthesis of Ammonia*; Gjellerup: Kopenhagen, Denmark, 1968.
15. Waugh, K.C.; Butler, D.; Hayden, B.E. The mechanism of the poisoning of ammonia synthesis catalysts by oxygenates O_2, CO and H_2O: An in situ method for active surface determination. *Catal. Lett.* **1994**, *24*, 197–210. [CrossRef]
16. Schütze, J.; Mahdi, W.; Herzog, B.; Schlögel, R. On the structure of the activated iron catalyst for ammonia synthesis. *Top. Catal.* **1994**, *1*, 195–214. [CrossRef]
17. Waugh, K.C.; Butler, D.; Hayden, B.E. On the mechanism of poisoning and promotion of ammonia synthesis. *Top. Catal.* **1994**, *1*, 295–301. [CrossRef]
18. Herzog, B.; Herein, D.; Schlögl, R. In situ X-ray powder diffraction analysis of the microstructure of activated iron catalysts for ammonia synthesis. *Appl. Catal. A Gen.* **1996**, *141*, 71–104. [CrossRef]
19. Rosowski, F.; Muhler, M. The influence of oxygen poisoning on a multiply promoted Iron catalyst used for ammonia synthesis: A temperature-programmed desorption and reaction study. In *Dynamics of Surfaces and Reaction Kinetics in Heterogeneous Catalysis*; Studies in Surface Science and Catalysis; Froment, G., Waugh, K., Eds.; Elsevier: Amsterdam, The Netherlands, 1997; Volume 109, pp. 111–120.

20. Nielsen, P.E.H. Poisoning of Ammonia Synthesis Catalysts. In *Ammonia Catalysis and Manufacture*; Nielsen, A., Ed.; Springer: Berlin/Heidelberg, Germany, 1995; pp. 191–198.
21. Nrøskov, J.K.; Stoltze, P. Elementary Steps and Mechanisms: Microkinetics: Theoretical Modeling of Catalytic Reactions. In *Handbook of Heterogeneous Catalysis*; Ertl, G., Knözinger, H., Schüth, F., Weitkamp, J., Eds.; Wiley-VCH Verlag: Hoboken, NJ, USA, 2008; pp. 1479–1489.
22. Hinrichsen, O.; Rosowski, F.; Muhler, M.; Ertl, G. The microkinetics of ammonia synthesis catalyzed by cesium-promoted supported ruthenium. *Chem. Eng. Sci.* **1996**, *51*, 1683–1690. [CrossRef]
23. Nam, Y.; Hudgins, R.; Silveston, P. Storage models for ammonia synthesis over iron catalyst under periodic operation. *Chem. Eng. Sci.* **1990**, *45*, 3111–3121. [CrossRef]
24. Dumesic, J.A.; Trevino, A.A. Kinetic simulation of ammonia synthesis catalysis. *J. Catal.* **1989**, *116*, 119–129. [CrossRef]
25. Kirkerød, T.; Skaugset, P. *Abstracts of IV Nordic Symposium on Catalysis*; Springer Science & Business Media: Trondheim, Norway, 1991.
26. Stegehake, C.; Riese, J.; Grünewald, M. Aktueller Stand zur Modellierung von Festbettreaktoren und Möglichkeiten zur experimentellen Validierung. *Chem. Ing. Technol.* **2018**, *90*, 1739–1758. [CrossRef]
27. Räuchle, K.; Plass, L.; Wernicke, H.J.; Bertau, M. Methanol for Renewable Energy Storage and Utilization. *Energy Technol.* **2016**, *4*, 193–200. [CrossRef]